RECORDSOF CHEMICAL SCIENCES

Optimization of Methylene Blue Photocatalytic Degradation over TiO2 P25 via Central Composite Design: Kinetic and Statistical Analysis

[1]*Abubakar Hamisu, [2]Auwal Yusha'u and [2]Kamaluddeen Sulaiman Kabo

Accepted: 11th March, 2025
Published: 29th April, 2025

1. Department of Chemistry, Kano University of Science and Technology Wudil, 3244 Kano, Nigeria.
2. Department of Chemistry, Federal University Dutsin-Ma, P.M.B 5001, Katsina State,

**Corresponding Author:*
Abubakar Hamisu
ababakary@gmail.com

FRsCS Vol. 4 No. 1 (2025)
Official Journal of Dept. of Chemistry, Federal University of Dutsin-Ma, Katsina State.
http://rscs.fudutsinma.edu.ng

ISSN (Online): 2705-2362
ISSN (Print): 2705-2354

https://doi.org/10.33003/frscs_2025_0401/11

Abstract

Photocatalytic degradation of methylene blue (MB) dye over TiO_2 metal oxide under UV radiations was optimized using a central composite design of response surface methodology. The effect of TiO_2 loading, MB initial concentration, and pH were studied in the range the 0.25-2 g/L, 15–35, and 2.5-8.5 ppm, respectively. The cubic model was suggested for the response because is more reliable and accurate than the quadratic model. The influence of three operational parameters (catalyst loading, initial MB concentration, and pH) was examined to maximize the photocatalyst performance. The significance of the model and regression coefficients was tested by the analysis of variance. Optimal conditions obtained from statistical analysis at catalyst loading of 1 gL-1, initial MB concentration of 25 mgL-1 and pH of 2.5 have shown MB percentage degradation of 67.47. The kinetics of the photocatalytic degradation of MB dye over TiO_2 under UV light (3 W) at a wavelength of 253 nm was nicely followed by pseudo-first-order kinetic. Moreover, the results predicted by the models were found to be in good agreement with those obtained by performing experiments (R2 = 0.9993 and Adj-R2= 0.9542).

Keywords: Response surface methodology (RSM), TiO_2 catalyst, Methylene Blue Dye, Kinetics

Introduction

Securing sufficiently clean water can be achieved by effective treatment of industrial wastewater. Among the various methods such as adsorption (Lin, Pan, Chen, Cheng, & Xu, 2009), filtration (Zagklis, Vavouraki, Kornaros, & Paraskeva, 2015), wet oxidation (Guo & Al-Dahhan, 2003) developed for wastewater treatment, heterogeneous photocatalysis has proved to be the most effective, economically feasible and an ideal method for the destruction of water pollutants (Hamisu, Adeyi, & Chijioke-Okere, 2021; Hamisu, Gaya, & Abdullah, 2020; Hamisu, Gaya, & Abdullah, 2021; Zhu et al., 2021). There is a consensus among researchers that TiO_2 is superior in photocatalysis than the other semiconductors (Menard, Drobne, & Jemec, 2011; Thiruvenkatachari, Vigneswaran, & Moon, 2008; Wang, Ma, Chen, Ji, & Zhao, 2011). TiO_2 has not only emerged as one of the most interesting materials in both homogeneous and heterogeneous catalysis but has also succeeded in getting the attention of material scientists and engineers in exploring distinctive semiconducting and catalytic properties (Ibhadon & Fitzpatrick, 2013). TiO_2 is one of the most widely investigated semiconducting metal oxides that exhibit photocatalytic activity and is used in a wide range of

applications (Chiu, Lee, & Hsieh, 2011; Perera et al., 2012; G. Wang et al., 2011). Long-term photostability, inertness to chemical environment, nontoxicity, relatively low cost, strong oxidizing ability, high optical properties, high specific surface area, and high photocatalytic degradation performance under longer wavelength(Chang et al., 2013; M Zulfiqar, Chowdhury, & Omar, 2018; Muhammad Zulfiqar, Omar, & Chowdhury, 2016) has made TiO_2 an important material in many practical applications such as photocatalysis, dye-sensitized solar cells, biomedical devices, electrochemical sensing, production of hydrogen, and emission of gas treatment(Chang et al., 2013; Roy, Berger, & Schmuki, 2011; Sreekantan & Wei, 2010; M Zulfiqar et al., 2018). On the other hand, TiO_2 nanotube (TNT) has particularly become attractive, because it combines unique geometrical features with a range of remarkable optical, electrical and chemical properties used in practical applications (Albu et al., 2008; Textor, Sittig, Frauchiger, Tosatti, & Brunette, 2001).

Experimental Design is of vital importance in achieving the optimum results with a minimum number of experiments conducted in a systematic way (Hamisu, Gaya, et al., 2021). The conventional univariate technique used to optimize the process parameters is incongruous with a large number of variables due to considerable time loss and cost requirements Furthermore, the major drawback of the univariate technique is the lack of interactive effects assessment of the influencing parameters (Sifontes et al.). Therefore, researchers are now approaching multivariate optimization techniques. Response surface methodology (RSM) is one of the design approaches for optimization and interactive effect assessment of the operational parameters (Sifontes et al.).

In this work, the photocatalytic kinetic MB dye removal was studied by measuring the % photodegradation of MB in aqueous solution under UV light irradiation. The heterogeneous catalyzed MB dye removal was optimized using response surface methodology (RSM), based on the central composite design (CCD) to determine the interaction between selected parameters (i.e., TiO_2 catalyst loading, MB dye initial concentration, and pH) as well as the optimal operating conditions for the process. However, different photocatalysts such as TiO_2, ZnO, ZrO_2, WO_3, Cu_2O, Fe_2O_3, ZnS, CuO, ZrS, SrO_2, CuS, and ZTO have been widely used for the photocatalytic degradation MB. But TiO_2 photocatalyst appeared as an efficient and promising candidate in the photocatalytic applications due to its chemical stability, non-toxic, low cost, environmentally friendly species, highest conversion efficiency, and photocatalytic activity compared to widely used abovementioned semiconductors photoresponsive catalysts (Hamisu, Gaya, et al., 2021).

MATERIALS AND METHODS

Materials

Commercial TiO_2 nanopowder ((P25, 80% anatase, and 20% rutile) was used as raw material and purchased from Sigma-Aldrich. Methylene blue (MB, 85 %), sulfuric acid (H_2SO_4, 95-98%), and sodium hydroxide

(NaOH, 98%), were purchased from R & M Chemicals.

Photocatalytic Experiment

The photocatalytic removal of MB was carried out in a photoreactor which is made of 300 mm long cylindrical stainless steel with a diameter of 80 mm and effective volume of 1.19 L. 3 W (E14 GMY China, wavelength = 253 nm) UV lamp was used as the light source. In a typical experiment, a solution containing an appropriate amount of MB and TiO_2 photocatalyst was added to the photoreactor. Where required, the pH of the solution was adjusted using NaOH and H_2SO_4 solution. During the reaction process, oxygen was continuously bubbled through the mixture to avoid a change in the concentration of dissolved oxygen. Aliquots of 10 ml test samples were let out of the sampling tab at periodic intervals of time, which were immediately filtered with a cellulose nitrate filter (0.45 μm) to separate TiO_2 from the solution. The residual concentration of the MB solution was measured at 465.4 nm using a Perkin Elmer Lambda 35 UV-vis spectrometer. The photoreactor used for the photocatalytic removal of MB over the TiO_2NPs under UV light irradiation is presented in Fig 1

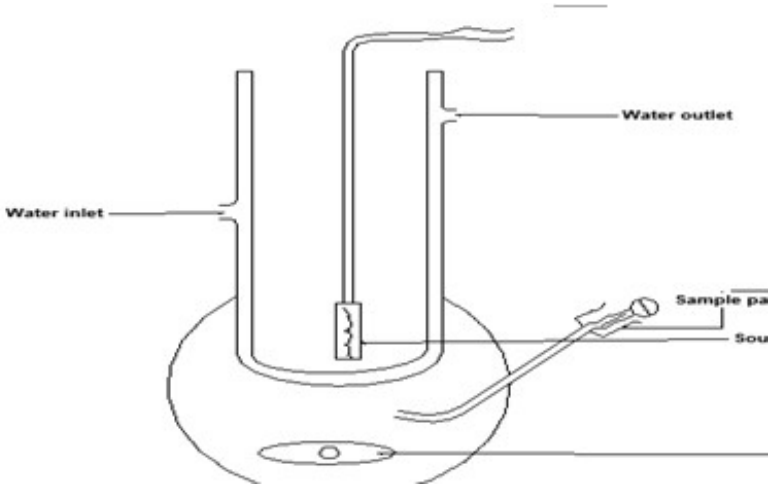

Fig 1. Schematic diagram of well immersion photoreactor

Design of Experiments

The photocatalytic MB removal TiO_2 metal oxide catalyst was modeled and optimized using response surface methodology (RSM), based on the central composite design (CCD). The effect of three independent variables (TiO_2 loading, initial concentration of MB, and pH) and their interactive impacts on the degradation of MB (as a response) were investigated in this study. In the study, a 2^3 central composite design was employed to fit the response. The CCD consists of three sets of points: center points, factorial points, and axial points. Table 1 shows the actual operating variable and their coded levels. The factorial points are located at the vertices of a cube box with coordinates which are a combination of -1(low value) and +1 (high value). The coordinate of the center points is 0,0,0. For axial points, star points were augmented to the factorial at a distance ± α = 1.68 along with center point

to make the design rotatable (as shown in Fig. 2). A total of 20 experiments was performed in this work, including eight experiments at factorial points, six experiments at the axial point, and six replications at central points, derived from the following equation (Eq. 5) (Jawad, Alkarkhi, & Mubarak, 2015).

$$N = 2^n + 2n + n_c = 2^3 + 2(3) + 6 = 20 \quad (5)$$

where N is the total number of experiments required, n is the number of factors and n_c is replications at central points. The experimental response factor is the % degradation (%D) of MB which was calculated using Eq. (6)

$$\%D = \frac{[MO]_o - [MO]_t}{[MO]_o} \times 100 \quad (6)$$

Table 1. Actual values and coded levels of operating variables.

Factor	Coded levels				
	-α	**Low**	**Middle**	**High**	**+α**
	-1.68	**-1**	**0**	**+1**	**+1.68**
[TiO_2] g/L	0.25	0.5	1	1.5	2
[MB] ppm	15	20	25	30	35
pH	2.5	4	5.5	7	8.5

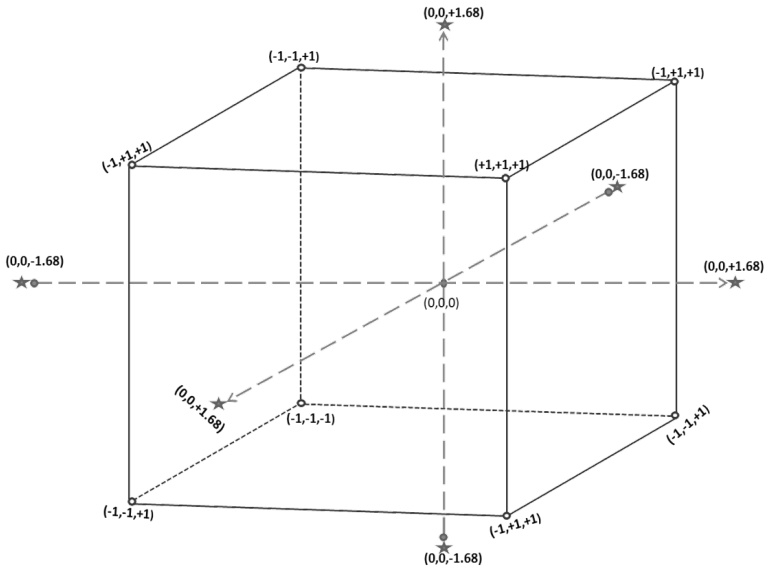

Fig 2. Graphical representation of 2^3 central composite designs (Hamisu, Gaya, et al., 2021).

RESULTS AND DISCUSSION

Photocatalytic Kinetics

To obtain relevant information, experiments were made (i) under UV irradiation without TiO_2 photocatalyst (photolysis) and (ii) in dark with TiO_2 photocatalyst (adsorption). The results showed that in both cases, no significant disappearance of methylene blue was observed (< 5% in both cases). The MB removal observed comes predominantly from photocatalytic degradation by TiO_2

photocatalyst, indicating that the system is working in a pure photocatalytic regime.

The degradation of MB carried out (Fig. 1) in this study can be fitted by pseudo-first-order kinetics (suggesting that a pseudo-first-order reaction model can be taken into consideration for describing the kinetic behavior). The pseudo-first-order kinetics can be represented by Eq. (4).

$$\ln\left(\frac{[MB]_o}{[MB]_t}\right) = kt \quad (4)$$

where $[MB]_t$ and $[MB]_o$ are the concentration (mg/L) at time t and when t = 0 respectively and k is the apparent reaction rate constant (expressed as min^{-1}). A plot of $\ln([MB]_o/[MB]_t)$ versus t gave a straight line with slope = k and R square value > 0.9 (Fig. 3). The apparent rate constants obtained from the pseudo-zero, first and second order kinetic is presented in Table 2. This shows that the data was nicely fitted in pseudo-first order with the coefficient of correlation (R^2=0.9995).

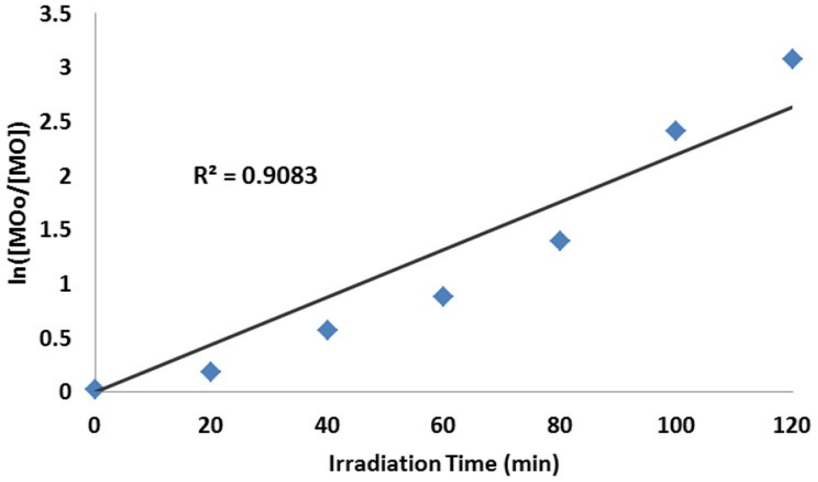

Fig 3. Pseudo-first-order graph of MB degradation.

Optimization experiments

The three independent variables (TiO_2 loading, MB dye initial concentration, and pH) effect and their interactive impacts on the degradation of MB (as a response) were investigated using the central composite design (CCD) approach, and response data were analyzed using Design-Expert version 6.0.6.

Table 2. Apparent rate constant (k_{app}) and coefficient of regression (R^2) according to the pseudo-zeroth, pseudo-first, and pseudo-second kinetic for photodegradation of MB over TiO_2 NPs

S/N	Model	Apparent rate constant (k_{app})	Correlation coefficient (R^2)
1	Pseudo-zeroth order	5.34 x10^{-2} moldm^{-3} s^{-1}	0.8999
2	Pseudo-first order	6.31 x10^{-2} s^{-1}	0.9994
3	Pseudo-second order	2.83 x10^{-2} mol^{-1}dm^3 s^{-1}	0.9549

Statistical analysis and response optimization

The degradation efficiency values obtained from an experiment (% D) were processed using a response surface module to obtain statistically valid predicted values. A cubic polynomial model was used to develop the mathematical relationship between the response and the independent process variables. The empirical relationships between the responses (%D) and independent variables are presented in Eq. (5)

$$\%D = 51.1 + 7.51[TiO2] - 7.14[MO] - 2.63(pH) - 9.87[TiO2]^2 - 9.34[MO]^2 - (pH)^2 - 1.5[TiO2] * [MO] - 4.25[TiO2] * (pH) + 4.25[MO] * (pH) - 0.76]TiO2]^3 + 3.89[MO]^3 - 2.31(pH)^3 + [TiO2] * [MO] * (pH) \quad (5)$$

Each coefficient of the variable in the equation estimates the change in mean response per unit increase in the associated independent variable when the other variable is held constant. The degradation efficiency (%D) obtained by the photocatalytic degradation process of MB has been predicted by Eq. (5) and the obtained results are presented in Table 3. It can be seen from the tables that, there is a good correlation between the experimental and predicted %degradation as testified by linear normal plot of residuals (Fig. A1, supplementary material). The majority of the points on the normal probability plot lie roughly in a straight line, so it can be concluded that the estimated effects are real and differ distinctly from noise

.

Table 3: The 2^3 central composite design matrix and the value of the response function (%Degradation)

				%Degradation	
Run	**[TiO_2] g/L**	**[MB] ppm**	**pH**	**Actual**	**Predicted**
1	1	25	5.5	52	51
2	1	25	5.5	49	51
3	0.5	20	4	56	57
4	0.5	30	7	20	21
5	1	35	5.5	33	31
6	0.25	25	5.5	16	14
7	0.5	20	4	25	26
8	1	25	5.5	49	51
9	1.5	30	4	32	33
10	1.5	20	7	23	24
11	0.5	20	7	21	22
12	1	25	8.5	30	28
13	2	25	5.5	34	32
14	1	25	5.5	51	51
15	0.5	30	4	19	20

16	1.5	30	7	28	29
17	1	25	5.5	52	51
18	1	15	5.5	20	18
19	1	25	5.5	53	51
20	1	25	2.5	61	59

The statistical significance of the CCD model was assessed by ANOVA. The ANOVA results are tabulated in Table 2. The results revealed that the obtained models can be successfully used to navigate the design space. The R^2 value was found to be 0.9783 which is close to 1. The R^2 values reveal that only about 2.17 % of the variation for MB degradation efficiency is not explained by the model. This observation was confirmed by comparing the experimental values against the predicted responses by the model for the percentage degradation of MB (Fig. 4).

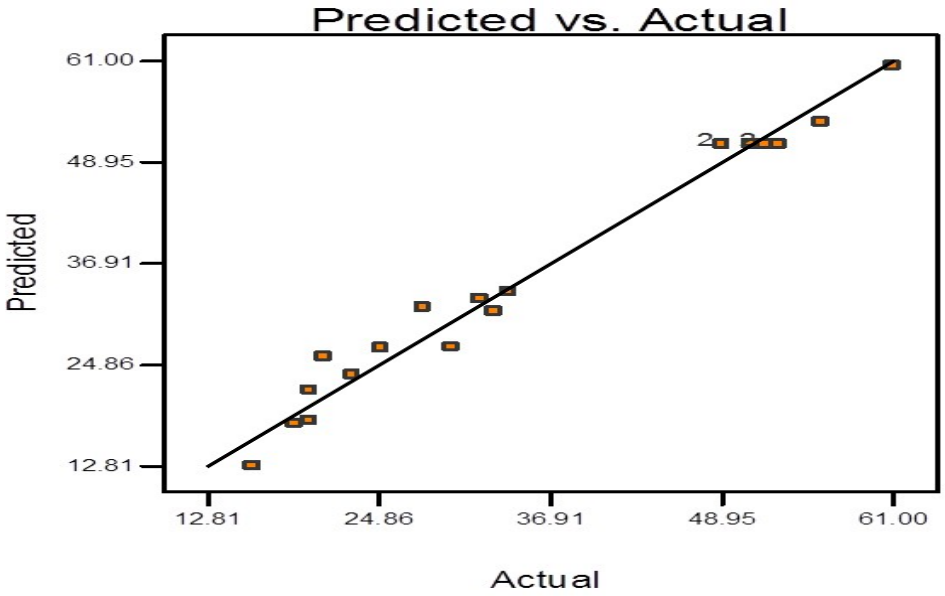

Fig. 4. Comparison of the experimental results of degradation efficiency with the predicted values by the CCD model.

For the fact that, in a system with a different number of independent variables, adjusted R^2 (Adj-R^2) is more suitable for evaluating the model goodness of fit (Jawad et al., 2015). In this respect, the Adj-R^2 value was found to be 0.9542 which is also close to 1. The model's Prob > F in the table is less than 0.05 which shows that predicted degradation efficiencies are not influenced at a 95 % confidence level. In any experiment, the minimum adequate precision desirable is a value > 4. In this study, the adequate precision is 20.103 which confirms the adequate significance of the model. Also, from Table 4, the high model F-value of 41.35 reveals that the model is significant. Furthermore, the residuals analysis (difference between the

observed and the predicted response value) also gives useful information about the model's goodness of fit. The normal probability plots show whether the residuals follow a normal distribution, in which the points will follow a straight line (Alidokht, Khataee, Reyhanitabar, & Oustan, 2011; Jawad et al., 2015). The plot of the normal probability of the residual for MB is shown in Fig. 5. The trend depicted in this figure reveals a reasonably well-behaved residual of MO and that the residual is normally distributed and resembles a straight line.

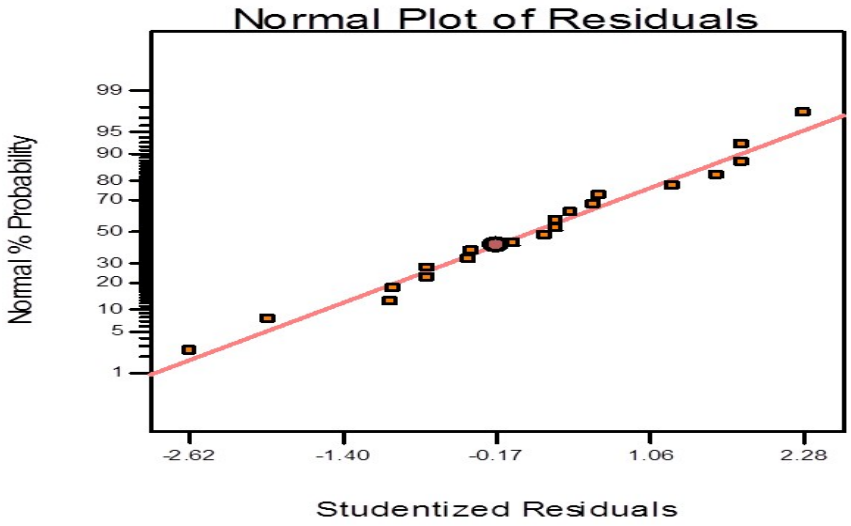

Fig. 5. Normal probability plots

Effect of operational variables on the response.

The influence of individual studied variables, comprising TiO_2 catalyst loading (A), MB dye initial concentration (B), and pH (C) on the MB removal as the response, was studied by perturbation plots. The perturbation plot utilizes the model terms to visualize the effect of each factor deviation from the reference point on the response. It can be employed to explore the most significant factors in the response. A steep slope or curvature of the plot reveals that the response is sensitive to that variable, whereas, a relatively plane line indicates insensitivity of the response to change in that particular factor (Jawad et al., 2015). Fig. 6 depicts the perturbation plot of MB moval. It can be seen from the figure, that the TiO_2 catalyst loading curve displays high steep curvature followed by MB initial concentration indicating TiO_2 loading is the most influential factor followed by MB initial concentration. On the other hand, pH curve shows low curvature indicating this factor has a slight effect on the response. These observations were confirmed by the coefficients of the model terms in Eq. 6. The coefficients of model terms, suggest that TiO_2 catalyst loading with a coefficient of 7.51 positive impact on degradation efficiency. And, the MB initial concentration has a more prominent

negative impact (-7.14) followed by pH with a coefficient of 2.630.

Table 4. ANOVA for cubic models

Source	Sum of square	DF	Mean Square	F value	Prop>F
Model	4186.48	13	322.04	41.35	< 0.0001
A	160.44	1	160.44	20.60	0.0039
B	144.88	1	144.88	18.60	0.0050
C	20.62	1	20.62	2.65	0.00019
A	1403.30	1	1403.30	180.20	< 0.0001
B	1256.52	1	1256.52	161.35	< 0.0001
C	98.93	1	98.93	12.70	0.0119
AB	18.00	1	18.00	2.31	0.1792
AC	144.50	1	144.50	18.56	0.0051
BC	144.50	1	144.50	18.56	0.0051
A	6.48	1	6.48	0.83	0.3968
B	167.75	1	167.75	21.54	0.0035
C	58.91	1	58.91	7.56	0.0333
ABC	72.00	1	72.00	9.25	0.0228
Residual	46.72	6	7.79	-	-
Lack of	32.72	1	32.72	11.69	0.0189
Fit	14.00	5	2.80	-	-
Pure Error					

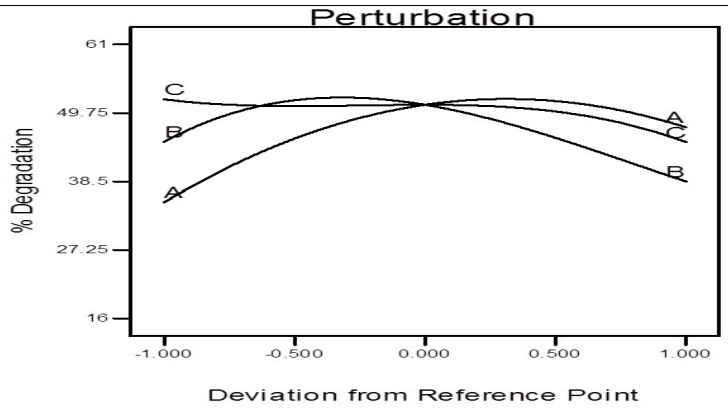

Figure. 6. Perturbation plots for MB degradation efficiency. (A: TiO_2 catalyst loading, B: pH, C: H_2O_2 concentration).

To study the interactive effect of the operational variables on the MB removal the response, three-dimensional surfaces, and two-dimensional contours were plotted and presented in Fig. 14. The figures were obtained by keeping one variable constant at the center level and the other two varying within the experimental ranges. As can be

seen, the percentage degradation of MB increases with an increase in TiO_2 up to 1g/L and decreases with a further addition of TiO_2 (Figure 7 A and C). Also, the % degradation of MB increases with an increase in [MB] up to 25 ppm which decreases above this concentration (Fig. 7 A and B). It was found that pH has a hurt effect on the %degradation of MB in which the % degradation decreases with an increase in pH (Fig. 7 B and C). The result showed that the highest % degradation was found in acidic conditions (pH =2.5) with optimum TiO_2 loading of 1g/L and initial concentration of 25 ppm.

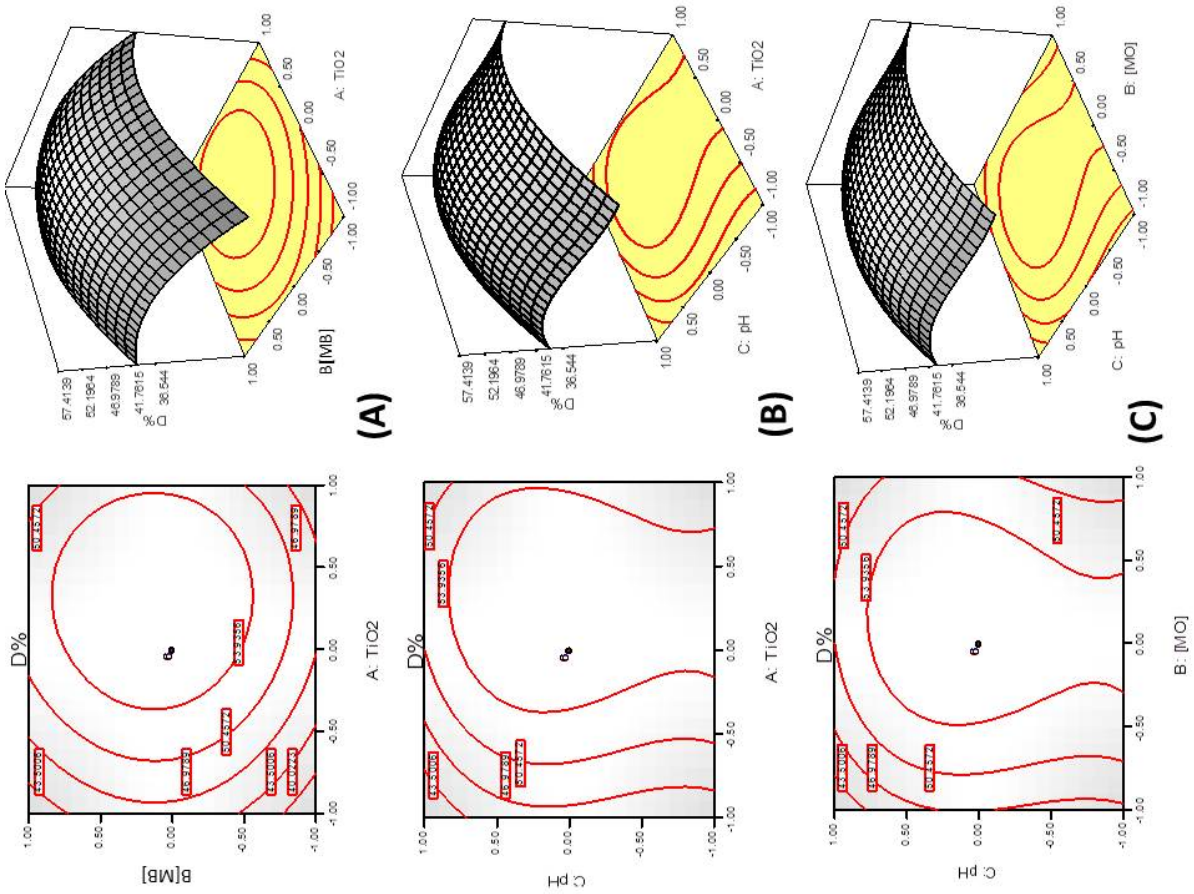

Figure 7. The response surface of MB % degradation as a function of (A) [MB] and [TiO_2], (B) pH and [MB] (C) pH and [TiO_2] (Irradiation time = 60 min).

CONCLUSION

The MB dye is decolorized by heterogeneous photocatalysis. The cubic model was found to be suitable for expressing the relationship between response variables and independent operating parameters (i.e. TiO_2 loading, MB initial concentration, and pH). The optimization goal for maximum MB dye removal for operating parameters within an experimental range was determined as the concentration of TiO_2: 1 g/L, MB dye initial concentration: 25 ppm, pH: 2.5. The heterogeneously catalyzed MB degradation on the TiO_2 metal oxide was found to follow pseudo-first order kinetic with R^2 value > 0.9. Furthermore, the visible-light catalysts could be used to address pH/UV limitations

REFERENCES

Albu, S. P., Ghicov, A., Aldabergenova, S., Drechsel, P., LeClere, D., Thompson, G. E., . . . Schmuki, P. (2008). Formation of double-walled TiO2 nanotubes and robust anatase membranes. *Advanced Materials, 20*(21), 4135-4139.

Alidokht, L., Khataee, A. R., Reyhanitabar, A., & Oustan, S. (2011). Cr (VI) immobilization process in a Cr-spiked soil by zerovalent iron nanoparticles: optimization using response surface methodology. *CLEAN–Soil, Air, Water, 39*(7), 633-640.

Chang, W.-T., Hsueh, Y.-C., Huang, S.-H., Liu, K.-I., Kei, C.-C., & Perng, T.-P. (2013). Fabrication of Ag-loaded multi-walled TiO 2 nanotube arrays and their photocatalytic activity. *Journal of Materials Chemistry A, 1*(6), 1987-1991.

Chiu, W.-H., Lee, K.-M., & Hsieh, W.-F. (2011). High-efficiency flexible dye-sensitized solar cells by multiple electrophoretic depositions. *Journal of Power Sources, 196*(7), 3683-3687.

Guo, J., & Al-Dahhan, M. (2003). Catalytic wet oxidation of phenol by hydrogen peroxide over pillared clay catalyst. *Industrial & Engineering Chemistry Research, 42*(12), 2450-2460.

Hamisu, A., Adeyi, A. A., & Chijioke-Okere, M. (2021). Preparation and visible light-catalytic activity of cadmium doped titania nanotube.

Hamisu, A., Gaya, U., & Abdullah, A. H. (2020). A Novel Poly (vinyl alcohol) Post-precipitation Template Synthesis and Property Tuning of Photoactive Mesoporous Nano-TiO2. *Physical Chemistry Research, 8*(2), 281-295.

Hamisu, A., Gaya, U. I., & Abdullah, A. H. (2021). Bi-Template Assisted Sol-Gel Synthesis of Photocatalytically-Active Mesoporous Anatase TiO2 Nanoparticles.

Ibhadon, A. O., & Fitzpatrick, P. (2013). Heterogeneous photocatalysis: recent advances and applications. *Catalysts, 3*(1), 189-218.

Jawad, A. H., Alkarkhi, A. F. M., & Mubarak, N. S. A. (2015). Photocatalytic decolorization of methylene blue by an immobilized TiO2 film under visible light irradiation: optimization using response surface methodology

(RSM). *Desalination and Water Treatment, 56*(1), 161-172. doi: 10.1080/19443994.2014.934736

Lin, K., Pan, J., Chen, Y., Cheng, R., & Xu, X. (2009). Study the adsorption of phenol from aqueous solution on hydroxyapatite nanopowders. *Journal of Hazardous materials, 161*(1), 231-240.

Menard, A., Drobne, D., & Jemec, A. (2011). Ecotoxicity of nanosized TiO2. Review of in vivo data. *Environmental Pollution, 159*(3), 677-684.

Perera, S. D., Mariano, R. G., Vu, K., Nour, N., Seitz, O., Chabal, Y., & Balkus Jr, K. J. (2012). Hydrothermal synthesis of graphene-TiO2 nanotube composites with enhanced photocatalytic activity. *ACS Catalysis, 2*(6), 949-956.

Roy, P., Berger, S., & Schmuki, P. (2011). TiO2 nanotubes: synthesis and applications. *Angewandte Chemie International Edition, 50*(13), 2904-2939.

Sifontes, A. B., Rosales, M., M, F. J., #233, ndez, Oviedo, O., & Zoltan, T. (2013). Effect of calcination temperature on structural properties and photocatalytic activity of ceria nanoparticles synthesized employing chitosan as template. *J. Nanomaterials, 2013*, 1-1. doi: 10.1155/2013/265797

Sreekantan, S., & Wei, L. C. (2010). Study on the formation and photocatalytic activity of titanate nanotubes synthesized via hydrothermal method. *Journal of Alloys and Compounds, 490*(1-2), 436-442.

Textor, M., Sittig, C., Frauchiger, V., Tosatti, S., & Brunette, D. M. (2001). Properties and biological significance of natural oxide films on titanium and its alloys *Titanium in medicine* (pp. 171-230): Springer.

Thiruvenkatachari, R., Vigneswaran, S., & Moon, I. S. (2008). A review on UV/TiO 2 photocatalytic oxidation process (Journal Review). *Korean Journal of Chemical Engineering, 25*(1), 64-72.

Wang, G., Wang, H., Ling, Y., Tang, Y., Yang, X., Fitzmorris, R. C., . . . Li, Y. (2011). Hydrogen-treated TiO2 nanowire arrays for photoelectrochemical water splitting. *Nano letters, 11*(7), 3026-3033.

Wang, Z., Ma, W., Chen, C., Ji, H., & Zhao, J. (2011). Probing paramagnetic species in titania-based heterogeneous photocatalysis by electron spin resonance (ESR) spectroscopy—a mini review. *Chemical Engineering Journal, 170*(2-3), 353-362.

Zagklis, D. P., Vavouraki, A. I., Kornaros, M. E., & Paraskeva, C. A. (2015). Purification of olive mill wastewater phenols through membrane filtration and resin adsorption/desorption. *Journal of Hazardous materials, 285*, 69-76.

Zhu, X., Zhou, Q., Xia, Y., Wang, J., Chen, H., Xu, Q., . . . Chen, S. (2021). Preparation and Characterization of Cu-doped TiO2 nanomaterials with Anatase/rutile/brookite Triphasic

Structure and their Photocatalytic Activity.

Zulfiqar, M., Chowdhury, S., & Omar, A. (2018). Hydrothermal synthesis of multiwalled TiO2 nanotubes and its photocatalytic activities for Orange II removal. *Separation Science and Technology, 53*(9), 1412-1422.

Zulfiqar, M., Omar, A. A., & Chowdhury, S. (2016). *Synthesis and characterization of single-layer TiO2 nanotubes.* Paper presented at the Advanced Materials Research.